A Novel Method for Quantifying the In-Vivo Mechanical Effect of Material Injected Into a Myocardial Infarction

Jonathan F. Wenk, PhD, Parastou Eslami, MS, Zhihong Zhang, MS, Chun Xu, PhD, Ellen Kuhl, PhD, Joseph H. Gorman III, MD, J. Daniel Robb, MBBS, Mark B. Ratcliffe, MD, Robert C. Gorman, MD, and Julius M. Guccione, PhD

Departments of Surgery and Bioengineering, University of California, San Francisco; Department of Veterans Affairs Medical Center, San Francisco; Gorman Cardiovascular Research Group, University of Pennsylvania, Philadelphia, Pennsylvania; and Department of Mechanical Engineering, Stanford University, Palo Alto, California

Background. **Infarcted regions of myocardium exhibit functional impairment ranging in severity from hypokinesis to dyskinesis. We sought to quantify the effects of injecting a calcium hydroxyapatite-based tissue filler on the passive material response of infarcted left ventricles.**

Methods. **Three-dimensional finite element models of the left ventricle were developed using three-dimensional echocardiography data from sheep with a treated and untreated anteroapical infarct, to estimate the material properties (stiffness) in the infarct and remote regions. This was accomplished by matching experimentally determined left ventricular volumes, and minimizing radial strain in the treated infarct, which is indicative of akinesia. The nonlinear stress-strain relationship for the diastolic myocardium was anisotropic with respect to the local muscle fiber direction, and an elastance model for active fiber stress was incorporated.**

Results. **It was found that the passive stiffness parameter, C, in the treated infarct region is increased by nearly 345 times the healthy remote value. Additionally, the average myofiber stress in the treated left ventricle was significantly reduced in both the remote and infarct regions.**

Conclusions. **Overall, injection of tissue filler into the infarct was found to render it akinetic and reduce stress in the left ventricle, which could limit the adverse remodeling that leads to heart failure.**

(Ann Thorac Surg 2011;92:935–41)

Recent studies of the biomechanical response of the left ventricle (LV) to myocardial infarction (MI) have identified infarct expansion (ie, stretching) as an important phenomenon that both initiates and sustains a progressive pathologic process that ultimately results in LV dilation, loss of global contractile function, symptomatic heart failure, and death. This maladaptive response is termed infarction-induced ventricular remodeling and is a complex process that is, in its initial phase, an almost completely mechanical problem manifest by abnormal myocardial stress patterns; however, with time these abnormal stress distributions lead to inherent biologic changes in the myocardium that become difficult to reverse by any means once established [1–5].

Awareness of the progressive nature of MI-induced LV remodeling and the relatively poor outcomes achieved with therapy for end-stage heart failure has led to increasing interest in developing early post-MI therapies intended to limit adverse remodeling.

The finite element (FE) method is the most versatile approach for computing myocardial stress and strain distributions in the LV. The FE models of the LV that incorporate myocardial contractility have been described and used to determine the effect of myocardial infarction on structure and function [6–8]. Additionally, the efficacy of various surgical procedures has been simulated with the FE method [9, 10].

Finite element models have also been used to investigate the effects of injecting biocompatible material into the wall of the LV to combat the progression of heart failure [11, 12]. Experimental studies by Ryan and associates [13] and Ifkovits and associates [14] have used large-animal models to examine the effects of injecting tissue filler and hydrogels into the infarcted LV, respectively. A review of biomaterial injection therapy for treating heart failure has recently been published [15].

In the current study, using an ovine infarct model, we tested the hypothesis that eliminating dyskinesia by infarct stiffening reduces LV stress and limits adverse remodeling. A commercially available reactive tissue filler agent was used to stiffen the infarct. The material was injected into the infarct immediately and resulted in an akinetic infarct at 8 weeks after infarction. The FE models were then created from contoured three-dimensional echocardiographic (3DE) images for an untreated (control) and treated animal, to estimate the

Accepted for publication April 26, 2011.

Address correspondence to Dr Guccione, Division of Surgical Services (112D), San Francisco Veterans Affairs Medical Center, 4150 Clement St, San Francisco, CA 94121; e-mail: guccionej@surgery.ucsf.edu.

Published by Elsevier Inc

0003-4975/$36.00
doi:10.1016/j.athoracsur.2011.04.089

material properties in the infarct and remote regions. This was accomplished by matching experimentally determined LV volumes, and minimizing radial strain in the treated infarct, which is indicative of akinesia. Two sheep were analyzed to demonstrate the methodology of model generation and numerical simulation from 3DE. A detailed description of the experimental measurements, taken from a large cohort of animals, can be found in the companion paper to this work, presented by Morita and colleagues [16].

Material and Methods

The animals used in this work received care in compliance with the protocols approved by the Institutional Animal Care and Use Committee at the University of Pennsylvania in accordance with the guidelines for humane care (National Institutes of Health Publication 85-23, revised 1996).

Experimental Measurements

The animal model has been described previously [17]. Briefly, two adult 40-kg Dorset sheep underwent ligation of the left anterior descending and second diagonal coronary artery that resulted in an infarction of approximately 20% of the LV mass at the anteroapex. Owing to the absence of collateral vessels, the demarcation between the infarct and healthy myocardium is quite distinct and visible during thoracotomy. The infarct region of one sheep was injected with 2.6 cc of a calcium hydroxyapatite-based tissue filler agent (Radiesse; Bioform Medical, San Mateo, CA) distributed over 20 evenly spaced injections, resulting in an akinetic infarct [13]. These injections were made directly into the myocardium. The second animal was used as a control (no tissue filler injection), resulting in a dyskinetic infarct. Further details about the injection procedure can be found in Morita and associates [16].

At 8 weeks post-MI, epicardial real-time 3DE was performed using a Philips iE33 platform with a 2-7 MHz matrix array real-time 3D ultrasound probe (Philips X7-2; Philips, Bothell, WA). Full-volume 3D datasets were acquired and postprocessed. After the 3D image was analyzed at end diastole (ED) and end systole (ES), on a dedicated work station, the resulting contour points were used to calculate the chamber volumes and generate the geometric surface data for the FE models. The contour points for the treated and control animals are shown in Figure 1A and 1B. Mitral and aortic valve function was normal in both animals.

Finite Element Models

The FE models were generated using early diastole as the initial unloaded reference state, since the LV pressure is lowest at this point and therefore stress is at a minimum. The infarct and remote regions were determined from the LV 3DE data points. In the case of the control animal, the boundary between the infarct and remote region was estimated by assessing the transition in wall thickness between the two regions [18]. For the treated animal, the boundary between the remote and akinetic region was created by overlapping the endocardial contours at ED and ES to determine where the wall does not move, indicating akinesia. In each case, the boundary was defined using 3D spline curves. Surface meshes were then created from the contour data points to replicate the in vivo geometry (Rapidform; INUS Technology, Sunnyvale, CA).

Volumetric meshes were generated by filling the space between the endocardial and epicardial surfaces with 8-node trilinear brick elements (Truegrid; XYZ Scientific Applications, Livermore, CA). Each 3D mesh consisted of three elements transmurally, 32 elements circumferentially, and 18 elements longitudinally, resulting in a total of 1,728 elements (Fig 2A and 2B). The remote region was assigned different material properties than the infarct region, representing the heterogeneous nature of the infarcted LV. The inner endocardial surface was lined with a layer of extremely soft linearly elastic shell elements to create an enclosed volume for LV volume calculations at ED and ES.

Cardiac myofiber angles of −37 degrees, 23 degrees, and 83 degrees were assigned at the epicardium, midwall, and endocardium, respectively, in the remote region [19]. At the infarct region, fiber angles were assigned to be 0 degrees, to use experimentally determined infarct material parameters with respect to this direction [20]. Nodes at the LV epicardial-basal edge were fully constrained, while the remaining basal nodes were restricted to displace in the circumferential-radial plane. The inner endocardial wall was loaded to the measured in vivo ED and ES LV pressures.

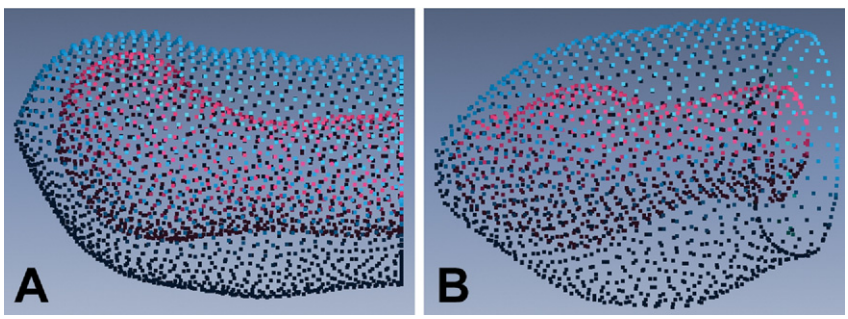

Fig 1. Contour points created from the three-dimensional echo images, which were used to generate the in vivo geometry for the (A) akinetic (treated) left ventricle and (B) the dyskinetic left ventricle.

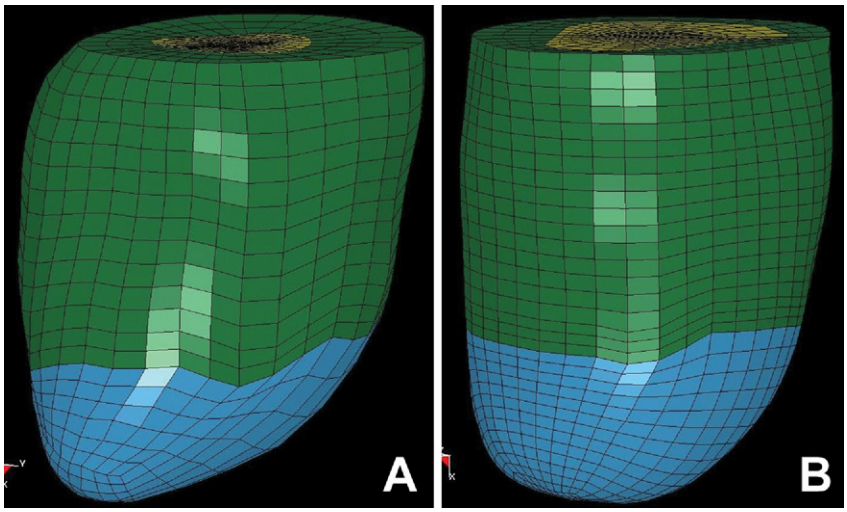

Fig 2. The volumetric mesh generated for the (A) akinetic (treated) left ventricle and (B) the dyskinetic left ventricle.

Diastolic and Systolic Material Properties

The material response was assumed to be nearly incompressible, transversely isotropic, and hyperelastic for both passive [21] and active myocardium [22]. An explicit FE solver (LS-DYNA; Livermore Software Technology, Livermore, CA) with a user-defined material subroutine was used to model the myocardium. The diastolic (passive) myocardial mechanics are described by the strain energy function, W, developed by Guccione and associates [21], which is transversely isotropic with respect to the local muscle fiber direction,

$$W = \frac{C}{2}\left\{\exp\left[b_f E_{11}^2 + b_t\left(E_{22}^2 + E_{33}^2 + E_{23}^2 + E_{32}^2\right) + b_{fs}\left(E_{12}^2 + E_{21}^2 + E_{13}^2 + E_{31}^2\right)\right] - 1\right\} \quad (1)$$

where C, b_f, b_t and b_{fs} are diastolic myocardial material parameters, E_{11} is the fiber strain, E_{22} is cross-fiber in plane strain, E_{33} is radial strain, and the rest are shear strains.

Systolic contraction was modeled by defining the second Piola-Kirchoff stress tensor as the sum of the passive stress derived from the strain energy function and an active fiber directional component, T_0, which is a function of time, t, peak intracellular calcium concentration, Ca_0, sarcomere length, l, and maximum isometric tension achieved at longest sarcomere length, T_{max} [22],

$$\mathrm{S} = pJ\mathrm{C}^{-1} + 2J^{-2/3}\mathrm{Dev}\left(\frac{\partial \widetilde{W}}{\partial \mathrm{C}}\right) + \mathrm{T}_0\{t,\ Ca_0, l, T_{\max}\} \quad (2)$$

where **S** is the second Piola-Kirchoff stress tensor, p is the hydrostatic pressure introduced as the Lagrange multiplier needed to enforce incompressibility, J is the Jacobian of the deformation gradient tensor, **C** is the right Cauchy-Green deformation tensor and the Dev is the deviatoric projection operator,

$$\mathrm{Dev}(\bullet) = (\bullet) - \frac{1}{3}([\bullet]{:}\mathrm{C})\ \mathrm{C}^{-1} \quad (3)$$

The deviatoric contribution of the strain energy function, W (Eq. 1), is $\widetilde{W}$. The strain energy function is decoupled into volumetric and deviatoric components due to the assumption of near incompressibility of the myocardium,

$$W = U(J) + \widetilde{W}(\widetilde{C}) \quad (4)$$

where U is the volumetric contribution.

The active fiber directional stress component is defined by a time-varying elastance model, which at ES, is reduced to [23],

$$T_0 = \frac{1}{2}T_{\max}\frac{Ca_0^2}{Ca_0^2 + ECa_{50}^2} \times\left(1 - \cos\left(\frac{0.25}{ml_R\sqrt{2E_{11} + 1 + b}} + 1\right)\pi\right) \quad (5)$$

where m and b are constants, and the length-dependent calcium sensitivity, ECa_{50}, is defined by,

$$ECa_{50} = \frac{(Ca_0)_{\max}}{\sqrt{\exp\left[B\left(l_R\sqrt{2E_{11} + 1} - l_0\right)\right] - 1}} \quad (6)$$

where B is a constant, $(Ca_0)_{\max}$ is the maximum peak intracellular calcium concentration, l_0 is the sarcomere length at which no active tension develops, and l_R is the stress-free sarcomere length. The material constants for active contraction were taken to be [24]: Ca_0 = 4.35 μmol/L, $(Ca_0)_{\max}$ = 4.35 μmol/L, B = 4.75 μm^{-1}, l_0 = 1.58 μm, m = 1.0489 s μm^{-1}, b = −1.429 s, and l_R, the sarcomere length in the unloaded configuration, was set at 1.85 μm. In accordance with biaxial stretching experiments [25] and FE analyses [8, 26], cross-fiber, in-plane stress equivalent to 40% of that along the myocardial fiber direction was added.

The diastolic material parameters, b_f, b_t, and b_{fs}, were assigned to be b_f = 3.5, b_t = 1.37, and b_{fs} = 1.24 for both cases. The passive stiffness parameters in the remote region, C_R, and the infarct, C_I, were determined by calibrating them such that the predicted ED LV volume matched the experimentally measured value. Similarly, the remote active contraction parameter, T_{max_R}, which represents the strength of contraction, was determined by matching the predicted ES LV volume to the mea-

sured value. The infarct active contraction was set to zero, as there are no contracting myocytes in the infarct.

In the case of the treated infarct, the material parameter search was subject to an additional criterion. The passive stiffness parameters were adjusted until the radial component of strain was nominally zero in the infarct, indicating akinesia, as well as matching the measured chamber volumes. This approach was adopted from Dang and associates [27], who used FE models, extrapolated from two-dimensional echocardiographic data, to examine akinetic infarcts. In our study, we have utilized data from full 3DE images, which eliminates the need for extrapolation.

Results

Hemodynamic and Echocardiographic Measurements

In the dyskinetic (control) case, the ED pressure was measured to be 9 mm Hg and the ES pressure was 93 mm Hg. The measured ED volume was 113.3 mL and the ES volume was 72.8 mL, which leads to an ejection fraction of 35%. In the akinetic (treated) case, the ED pressure was found to be 12 mm Hg and the ES pressure was 97 mm Hg. The ED volume was 48.4 mL and the ES volume was 22.8 mL, which is an ejection fraction of 53%.

Finite Element Output

The deformed states at ED and ES, obtained for the akinetic LV, are shown in Figure 3A and 3B, and the overlap of the endocardial surfaces at ED and ES is shown in Figure 3C. The passive stiffness for the akinetic case was estimated to be $C_R = 0.87$ kPa in the remote region and $C_I = 300$ kPa for the infarct region. The active contraction parameter was estimated to be $T_{max\_R} = 130$ kPa for the remote region and $T_{max\_I} = 0$ kPa for the infarct region (as stated previously). The akinesia was estimated by computing the average radial strain in the infarct region, which was found to be $e_{rr} = 0.0014$. This implies that on average the wall thickness in the infarct region changed by less than 0.14%.

In the dyskinetic LV case, the passive material properties were estimated to be $C_R = 3$ kPa and $C_I = 150$ kPa for the remote and infarct zones, respectively. The active contraction was found to be $T_{max\_R} = 500$ kPa for the remote and $T_{max\_I} = 0$ kPa for the infarct region. A summary of material properties described above is given in Table 1. Fiber stress distributions and regional average stress values for both cases are shown in Figure 4 and Table 2, respectively. The average ED fiber stress is nearly twice as high in the infarct of the untreated dyskinetic LV, whereas the average ES fiber stress is nearly 10 times higher in the infarct of the dyskinetic LV.

Comment

In the current study, we used contour data acquired from fully 3DE imaging to create FE models of two ovine hearts 8 weeks after large anteroapical infarction. One animal had infarct stiffening therapy with a reactive tissue filler agent and the other was an untreated control. The tissue filler initially limits infarct stretching and thinning by a mass effect, but over time it stimulates increased collagen deposition that maintains tissue thickness and stiffness even after most of the injected material has been absorbed [13].

The use of 3DE (as opposed to 2DE) data allowed for more realistic estimates of LV volumes and regional myocardial material properties compared with our previously published work [27].

Passive Material Properties

It was determined by Dang and associates [27] that for a noncontracting infarct to be akinetic, the passive stiffness must be greater than 285 times the normal healthy value.

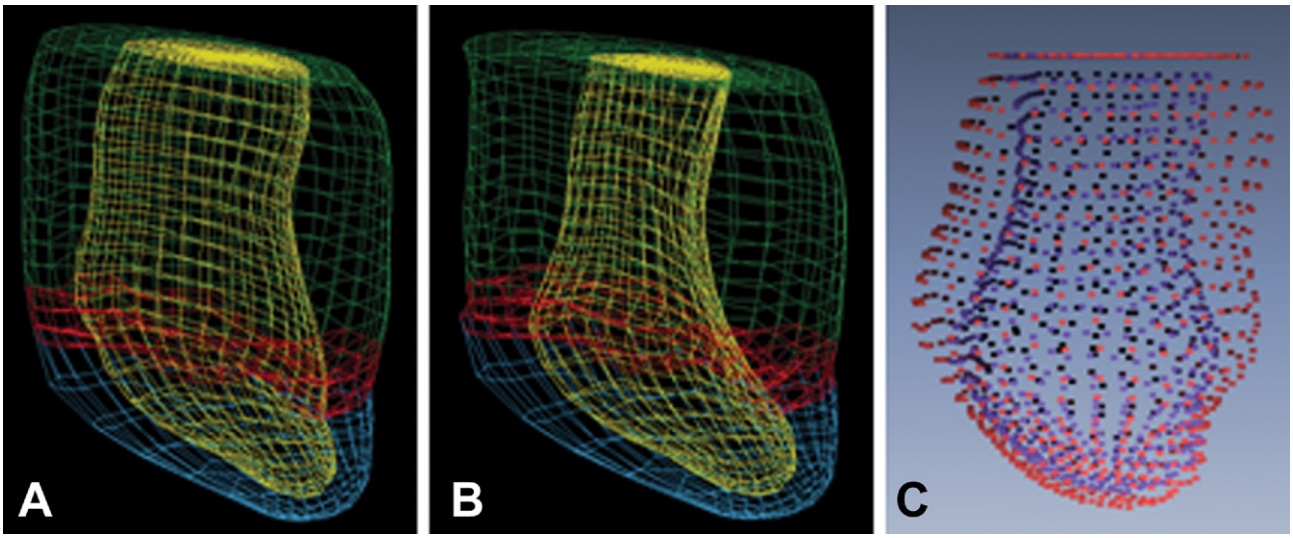

Fig 3. The model configuration of the akinetic (treated) case at (A) end diastole, (B) end systole, and (C) overlap and comparison of the endocardium at end systole and end diastole.

Table 1. Material Properties of Dyskinetic (Control) and Akinetic (Treated) Left Ventricle

	Passive Stiffness, C (kPa)		Active Contraction, T_{max} (kPa)	
	Remote	Infarct	Remote	Infarct
Control	3.0	150	500	0
Treated	0.87	300	130	0

kPa = kilopascal.

Table 2. Average Fiber Stress Values for Dyskinetic (Control) and Akinetic (Treated) Cases in Remote and Infarct Region at End Diastole and End Systole

	Average End-Diastolic Fiber Stress (kPa)		Average End-Systolic Fiber Stress (kPa)	
	Remote	Infarct	Remote	Infarct
Control	2.49	7.50	35.1	61.6
Treated	0.535	3.66	29.4	4.42

kPa = kilopascal.

In the current study, it was found that the tissue filler injection causes the passive stiffness to be 345 times greater than normal myocardium. Ifkovits and associates [14] also showed an increase in stiffness due to the injection of hyaluronic acid hydrogels into infarcted tissue. Morita and associates [16] performed experimental biaxial tensile tests on injected infarct tissue that showed that the peak strain in the longitudinal direction of the infarct was significantly reduced. This implies that the stiffness of the treated infarct has increased relative to the control case, as was also found in the current FE study.

In the control case, the passive stiffness was found to be 50 times higher in the infarct region than in the healthy remote region. This is the same order of magnitude increase as the values reported in similar studies of infarct modeling using the FE method [28, 29]. In many cases, the infarct is assumed to be 10 times stiffer than the remote, but it is possible for this ratio to be higher as there is variation between animals [30].

Stress Distribution and Ejection Fraction

It can be seen in Table 2 that the average fiber stress is higher overall in the dyskinetic (untreated) case. The maximum difference between the dyskinetic and akinetic case is the ES fiber stress in the infarct regions, where the injection of tissue filler reduced the stress by nearly 10 times. It can be seen in Figure 4 that there are stress concentrations at the boundary between the infarct and remote region that could lead to the progressive impairment of contracting myocytes in the borderzone region. It can also be seen that the wall thickness in the infarct region is much greater in the treated LV, also helping reduce stress. The effects of the injections were found to

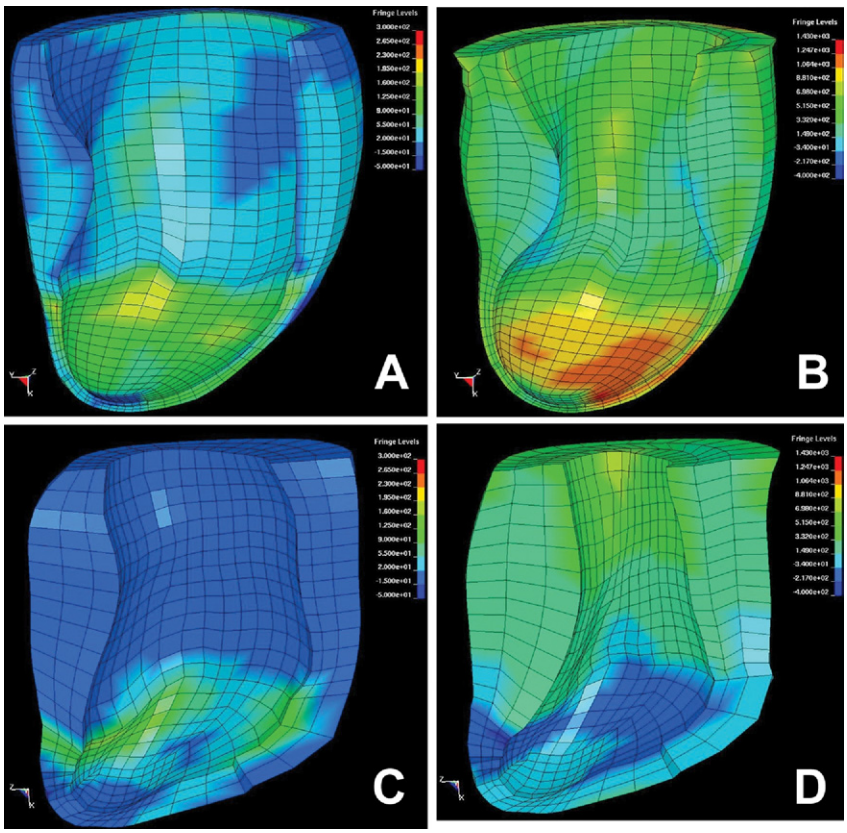

Fig 4. Fiber stress distribution in the lateral wall of the dyskinetic left ventricle at (A) end diastole and (B) end systole. Fiber stress distribution in the lateral wall of the akinetic (treated) left ventricle at (C) end diastole and (D) end systole. It should be noted that the color scales of the end diastole panels are the same, and the color scales of the end systole panels are the same.

be transmural throughout the entire infarct region, by inducing collagen production within the infarct tissue [16]. By eliminating the bulging that occurs during dyskinesis, the ejection fraction of the treated heart was 53%, which is close to a normally functioning heart [13]. Thus, both stress and ejection fraction are improved, relative to the untreated case.

Study Limitations

There are limitations in the current study. First, the treated infarct was assumed to be homogeneous, rather than modeling the distribution of injected material and tissue response separately. Second, only two animals were analyzed in the study to develop the modeling methodology; admittedly, the treatment animal was selected from a cohort of 11 animals in which it manifest the most benefit from injection of the material based on attenuation of LV dilation [16]. In the future, this method will be applied to a large cohort of animals to determine the statistical relevance. Finally, the validation of the models was based on matching experimental LV chamber volume, and in the case of the treated animal, the radial strain in the infarct region. In the future, this will be improved by computing myocardial strain from 3D magnetic resonance imaging, which will be compared with the FE simulation results.

In summary, we have presented a methodology for using 3DE images to generate FE models of an anteroapical infarct model. This was done to investigate the alterations to myocardial material properties due to the injection of calcium hydroxyapatite-based tissue filler. It was found that the passive stiffness value in the treated infarct region is increased by near 345 times the healthy value, and the thickness of the infarct wall is also increased. Overall, the injection of tissue filler was found to cause akinesia in the infarct and globally reduce stress in the LV, and that could limit adverse remodeling.

This work was supported by grants from the National Heart, Lung, and Blood Institute of the National Institutes of Health, Bethesda, MD (HL84431, HL86400, HL63348, HL77921, and HL99172). Drs Robert Gorman and Joseph Gorman are supported by individual Established Investigator Awards from the American Heart Association, Dallas, TX.

References

1. Eaton L, Weiss J, Bulkley B, et al. Regional cardiac dilatation after acute myocardial infarction. N Engl J Med 1979;300:57–62.
2. Erlebacher J, Weiss J, Weisfeldt M, et al. Early dilation of the infarcted segment in acute transmural myocardial infarction: role of infarct expansion in acute left ventricular enlargement. J Am Coll Cardiol 1989;4:201–8.
3. Jackson B, Gorman J, Moainie S, et al. Extension of border-zone myocardium in postinfarction dilated cardiomyopathy. J Am Coll Cardiol 2002;40:1160–7.
4. Jeremy R, Allman K, Bautovitch G, et al. Patterns of left ventricular dilation during the six months after myocardial infarction. J Am Coll Cardiol 1989;13:304–10.
5. St. John-Sutton M, Pfeffer M, Moye L, et al. Cardiovascular death and left ventricular remodeling two years after myocardial infarction: baseline predictors and impact of long-term use of captopril. Information from the Survival and Ventricular Enlargement (SAVE) trial. Circulation 1997;96:3294–9.
6. Dang AB, Guccione JM, Mishell JM, et al. Akinetic myocardial infarcts must contain contracting myocytes: finite-element model study. Am J Physiol Heart Circ Physiol 2005;288:H1844–50.
7. Guccione JM, Moonly SM, Moustakidis P, et al. Mechanism underlying mechanical dysfunction in the border zone of left ventricular aneurysm: a finite element model study. Ann Thorac Surg 2001;71:654–62.
8. Walker JC, Ratcliffe MB, Zhang P, et al. MRI-based finite-element analysis of left ventricular aneurysm. Am J Physiol Heart Circ Physiol 2005;289:H692–700.
9. Dang AB, Guccione JM, Zhang P, et al. Effect of ventricular size and patch stiffness in surgical anterior ventricular restoration: a finite element model study. Ann Thorac Surg 2005;79:185–93.
10. Walker JC, Ratcliffe MB, Zhang P, Wallace AW, Hsu EW, Saloner DA, Guccione JM. Magnetic resonance imaging-based finite element stress analysis after linear repair of left ventricular aneurysm. J Thorac Cardiovasc Surg 2008;135:1094–102.
11. Wall ST, Walker JC, Healy KE, et al. Theoretical impact of the injection of material into the myocardium: a finite element model simulation. Circulation 2006;114:2627–35.
12. Wenk JF, Wall S, Peterson, RC, et al. A method for automatically optimizing medical devices for treating heart failure: designing polymeric injection patterns. J Biomech Eng 2009; 131:121011.
13. Ryan LP, Jackson BM, Parish LM, et al. Regional and global patterns of annular remodeling in ischemic mitral regurgitation. Ann Thorac Surg 2007;84:553–9.
14. Ifkovits JL, Tous E, Minakawa M, et al. Injectable hydrogel properties influence infarct expansion and extent of postinfarction left ventricular remodeling in an ovine model. Proc Natl Acad Sci USA 2010;107:11507–12.
15. Nelson DM, Ma Z, Fujimoto KL, et al. Intra-myocardial biomaterial injection therapy in the treatment of heart failure: materials, outcomes and challenges. Acta Biomater 2011;7:1–15.
16. Morita M, Eckert CE, Matsuzaki K, et al. Modification of infarct material properties limits adverse ventricular remodeling. Ann Thorac Surg 2011;92:617–25.
17. Markovitz LJ, Savage EB, Ratcliffe MB, et al. Large animal model of left ventricular aneurysm. Ann Thorac Surg 1989; 48:838–45.
18. Moustakidis P, Maniar HS, Cupps BP, et al. Altered left ventricular geometry changes the border zone temporal distribution of stress in an experimental model of left ventricular aneurysm: a finite element model study. Circulation 2002;106(Suppl 1):168–75.
19. Omens JH, May KD, McCulloch AD. Transmural distribution of three-dimensional strain in the isolated arrested canine left ventricle. Am J Physiol Heart Circ Physiol 1991; 261:H918–28.
20. Moonly S. Experimental and computational analysis of left ventricular aneurysm mechanics [PhD thesis]. San Francisco, CA: University of California, San Francisco, with University of California, Berkeley, 2003.
21. Guccione JM, McCulloch AD, Waldman LK. Passive material properties of intact ventricular myocardium determined from a cylindrical model. J Biomech Eng 1991;113:42–55.
22. Guccione JM, Waldman LK, McCulloch AD. Mechanics of active contraction in cardiac muscle: part II—cylindrical models of the systolic left ventricle. J Biomech Eng 1993;115:82–90.
23. Tozeren A. Continuum rheology of muscle contraction and its application to cardiac contractility. Biophys J 1985;47:303–9.
24. Guccione JM, Costa KD, McCulloch AD. Finite element stress analysis of left ventricular mechanics in the beating dog heart. J Biomech 1995;28:1167–77.
25. Lin DH, Yin FC. A multiaxial constitutive law for mammalian left ventricular myocardium in steady-state barium contracture or tetanus. J Biomech Eng 1998;120:504–17.

26. Usyk TP, Mazhari R, McCulloch AD. Effect of laminar orthotropic myofiber architecture on regional stress and strain in the canine left ventricle. J Elasticity 2000;61:143–64.
27. Dang AB, Guccione JM, Mishell JM, et al. Akinetic myocardial infarcts must contain contracting myocytes: finite-element model study. Am J Physiol Heart Circ Physiol 2005;288:H1844–50.
28. Sun K, Zhang Z, Suzuki T, et al. Dor procedure for dyskinetic anteroapical left ventricular aneurysm fails to improve myocardial contractility in the borderzone. J Thorac Cardiovasc Surg 2010;140:233–9.
29. Sun K, Stander N, Jhun C-S, et al. A computationally efficient formal optimization of regional myocardial contractility in a sheep with left ventricular aneurysm. J Biomech Eng 2009;131:111001.
30. Walker JC, Ratcliffe MB, Zhang P, et al. MRI-based finite-element analysis of left ventricular aneurysm. Am J Physiol Heart Circ Physiol 2005;289:H692–700.

Southern Thoracic Surgical Association Fifty-Eighth Annual Meeting

Make plans now to attend the Fifty-Eighth Annual Meeting of the Southern Thoracic Surgical Association (STSA) on November 9–12, 2011, at the JW Marriott San Antonio Hill Country Resort in San Antonio, Texas. Please visit www.stsa.org to make hotel reservations and to learn more about the schedule of events.